


















RESEARCH ARTICLE OPEN ACCESS

Phenology Across Scales: An Intercontinental Analysis of Leaf-Out Dates in Temperate Deciduous Tree Communities

Nicolas Delpierre^{1,2}  | Suzon Garnier¹ | Hugo Treuil-Dussouet¹ | Koen Hufkens^{3,4,5}  | Jianhong Lin¹ | Colin Beier⁶ | Michael Bell⁷ | Daniel Berveiller¹ | Matthias Cuntz⁸  | Giulio Curioni⁹  | Kyla Dahlin¹⁰  | Sander O. Denham¹¹  | Ankur R. Desai¹²  | Jean-Christophe Domec¹³  | Kris M. Hart⁹  | Andreas Ibrom¹⁴  | Emilie Joetzjer⁸ | John King¹⁵ | Anne Klosterhalfen¹⁶  | Franziska Koebsch¹⁶ | Peter Mc Hale⁶ | Alexandre Morfin¹ | J. William Munger¹⁷  | Asko Noormets¹⁸ | Kim Pilegaard¹⁴  | Felix Pohl¹⁹  | Corinna Rebmann²⁰  | Andrew D. Richardson²¹ | David Rothstein¹⁰ | Mark D. Schwartz²²  | Matthew Wilkinson⁷  | Kamel Soudani¹

¹Université Paris-Saclay, CNRS, AgroParisTech, Ecologie Systématique et Evolution, Gif-sur-Yvette, France | ²Institut Universitaire de France (IUF), Paris, France | ³Institute of Geography, University of Bern, Bern, Switzerland | ⁴Oeschger Centre for Climate Change Research, University of Bern, Bern, Switzerland | ⁵BlueGreen Labs, Melsele, Belgium | ⁶College of Environmental Science and Forestry, State University of New York, Syracuse, New York, USA | ⁷Forest Research UK, Alice Holt, Surrey, UK | ⁸Université de Lorraine, AgroParisTech, INRAE, UMR Silva, Nancy, France | ⁹Birmingham Institute of Forest Research, School of Geography, Earth and Environmental Sciences, University of Birmingham, Birmingham, UK | ¹⁰Department of Geography, Environment, and Spatial Science, Michigan State University, East Lansing, Michigan, USA | ¹¹United States Department of Agriculture—Agricultural Research Service (USDA-ARS) Jornada Experimental Range, Las Cruces, New Mexico, USA | ¹²Department of Atmospheric and Oceanic Sciences, University of Wisconsin-Madison, Madison, Wisconsin, USA | ¹³Bordeaux Sciences Agro, INRAE ISPA, UMR 1391, Gradignan, France | ¹⁴DTU Sustain, Climate and Monitoring, Kgs. Lyngby, Denmark | ¹⁵Department of Forestry and Environmental Resources, North Carolina State University, Raleigh, North Carolina, USA | ¹⁶Bioclimatology, University of Göttingen, Göttingen, Germany | ¹⁷Department of Earth and Planetary Sciences and School of Engineering and Applied Sciences, Harvard University, Cambridge, Massachusetts, USA | ¹⁸Department of Ecology and Conservation Biology, Texas A&M University, College Station, Texas, USA | ¹⁹Helmholtz Centre for Environmental Research GmbH – UFZ, Leipzig, Germany | ²⁰IMK-TRO, Karlsruhe Institute of Technology, Karlsruhe, Germany | ²¹Center for Ecosystem Science and Society, School of Informatics, Computing and Cyber Systems, Northern Arizona University, Flagstaff, Arizona, USA | ²²Geography Department, University of Wisconsin-Milwaukee, Milwaukee, Wisconsin, USA

Correspondence: Nicolas Delpierre (nicolas.delpierre@universite-paris-saclay.fr)

Received: 21 November 2023 | **Revised:** 8 August 2024 | **Accepted:** 13 August 2024

Handling Editor: Jonathan Lenoir

Funding: The authors received no specific funding for this work.

Keywords: dominant trees | Europe | intra-community variability | leaf-out | North America | phenology | temperate forests

ABSTRACT

Aim: To quantify the intra-community variability of leaf-out (ICVLo) among dominant trees in temperate deciduous forests, assess its links with specific and phylogenetic diversity, identify its environmental drivers and deduce its ecological consequences with regard to radiation received and exposure to late frost.

Location: Eastern North America (ENA) and Europe (EUR).

Time Period: 2009–2022.

Major Taxa Studied: Temperate deciduous forest trees.

Methods: We developed an approach to quantify ICVLo through the analysis of RGB images taken from phenological cameras. We related ICVLo to species richness, phylogenetic diversity and environmental conditions. We quantified the intra-community variability of the amount of radiation received and of exposure to late frost.

This is an open access article under the terms of the [Creative Commons Attribution-NonCommercial-NoDerivs](https://creativecommons.org/licenses/by-nc-nd/4.0/) License, which permits use and distribution in any medium, provided the original work is properly cited, the use is non-commercial and no modifications or adaptations are made.

© 2024 The Author(s). *Global Ecology and Biogeography* published by John Wiley & Sons Ltd.

Results: Leaf-out occurred over a longer time interval in ENA than in EUR. The sensitivity of leaf-out to temperature was identical in both regions (−3.4 days per °C). The distributions of ICVLo were similar in EUR and ENA forests, despite the latter being more species-rich and phylogenetically diverse. In both regions, cooler conditions and an earlier occurrence of leaf-out resulted in higher ICVLo. ICVLo resulted in ca. 8% difference of radiation received from leaf-out to September among individual trees. Forest communities in ENA had shorter safety margins as regards the exposure to late frosts, and were actually more frequently exposed to late frosts.

Main Conclusions: We conducted the first intercontinental analysis of the variability of leaf-out at the scale of tree communities. North American and European forests showed similar ICVLo, in spite of their differences in terms of species richness and phylogenetic diversity, highlighting the relevance of environmental controls on ICVLo. We quantified two ecological implications of ICVLo (difference in terms of radiation received and exposure to late frost), which should be explored in the context of ongoing climate change, which affects trees differently according to their phenological niche.

1 | Introduction

1.1 | Intra-Community Variability of Leaf Phenology in Temperate Forests

The phenology of the tree canopy strongly influences the functioning of forests (Barr et al. 2007; Delpierre et al. 2009; Richardson et al. 2010) and of the climate system (Richardson et al. 2013) by modulating the exchange of matter and energy with the atmosphere. A wealth of study has been devoted to identify the environmental and biological drivers of spring leaf-out. These studies have highlighted the central roles of temperature and photoperiod (see Delpierre et al. 2016 for a review). Almost all these studies have focused on the average date of leaf-out in the ecosystem. Yet, when conducting phenological observations in a forest, one can observe a large inter-individual variability of leaf-out among conspecifics (Lechowicz 1984). In a preceding study, we showed that the average variability of leaf-out within a population of trees is 19 days, which corresponds to 75% of the variability observed at the scale of the continent (considered species were temperate oaks and beech, see Delpierre et al. 2017).

Such a wide range in leaf-out date could arise from phenology being a neutral trait for the tree, not affecting its fitness and therefore not being the object of natural selection (Lechowicz 1984). This idea is currently an object of debate, with little data documenting the link between phenology and fruit productivity (as a direct measure of fitness). Some studies have investigated the link between phenology and growth (an indirect measure of fitness), but their results are partly contradictory, with some showing no link between inter-annual variations of ring width indices and leaf phenology for a given tree (Čufar et al. 2015; Charlet de Sauvage et al. 2022) and others showing a globally significant, but not systematic, link between basal area increment and leaf phenology among dominant conspecifics in a given population (Delpierre et al. 2017). Leaving that debate aside, it is likely that the wide range of leaf-out dates observed in forests is due to the process of stabilising selection in which environmental conditions will impose limits to the acceptable variability achievable in phenological traits, while within-community interactions will favour inter-individual variability (Violle et al. 2012). In that context, fluctuating interactions and hazards may favour a large variability of phenological traits in a population (Alberto et al. 2011). For instance, individual trees

that leaf-out late will probably be advantaged in years with a late frost, but may logically be disadvantaged in years when early spring conditions are favourable (e.g., because their period of exposure to light will be shorter) or when pathogens flourish (Dantec et al. 2015). Ongoing climate change is accompanied by changes in the probability of exposure to late frost (Zohner et al. 2020), which could influence communities differently in areas where the probability is increasing (e.g., Europe, but see Lin, Rathgeber, and Delpierre 2024) than in areas where it is decreasing (e.g., North America).

The factors determining the intra-population variability of leaf-out have been little studied, but it is established that edaphic conditions (nature of the soil in Arend, Geßler, and Schaub 2016, soil water content in Delpierre et al. 2017), microclimate (e.g., local seasonal air temperature in Donnelly et al. 2017), genetic variability (Bontemps et al. 2015) and ontogeny (Vitasse 2013) are involved. Furthermore, the intra-population variability in leaf-out itself varies from year to year, depending on the prevailing micrometeorological conditions; the colder the temperature during leaf-out, the greater the intra-population variability (Denéchère et al. 2021; Delpierre et al. 2020).

The amplitude of leaf-out (i.e., the duration from the earliest to latest tree to leaf out) is likely to increase as one moves from the population to the community, encompassing a wider range of phenological niches. These niches are distributed vertically (e.g., dominant vs. understory tree species; Richardson et al. 2009) and horizontally (e.g., early vs. late species in the overstory, Cole and Sheldon 2017). The evolutionary history of species (i.e., genetic determinism) explains the inter-specific differences in leaf-out within a community (Lechowicz 1984). In this context, a more species-rich community would also be expected to have a greater phenological range, the phenological range of the community being composed of the specific phenological ranges (Figure S1). In addition to species richness, the phylogenetic diversity of communities deserves to be considered, as plants display a certain phylogenetic conservatism (whereby phylogenetically close species display similar phenological traits; Davies et al. 2013; Panchen et al. 2014). For example, one would expect a larger intra-community variability of leaf-out (ICVLo) in North American forests than in European forests, all else being equal, because they are more species rich (Liang et al. 2022; Latham and Ricklefs 1993) and display a higher phylogenetic diversity (Eiserhardt et al. 2015).

The ICVLo itself varies from year to year (Figure S1), probably in response to variations in environmental conditions. For instance, ICVLo is likely to be smaller during warm springs, as the accumulation of growing degree days occurs faster (Denéchére et al. 2021).

1.2 | Using Phenocams to Study the Intra-Community Variability of Leaf Phenology

A large part of the literature on forest leaf phenology is based on ground observation data. These data are historically the oldest and have been collected in national to continental databases (e.g., PEP725 Templ et al. 2018, NPN-usa Betancourt et al. 2007) that cover a period of several decades (e.g., from the 1950s in the PEP725 database). In the late 2000s, the use of ‘digital repeat photography’ to document the phenology of plant canopies became widespread (Richardson et al. 2007, 2009). These studies were initially based on the analysis of data obtained by automated photographic instruments, most often mounted on towers overhanging the canopy (i.e., phenological cameras or ‘phenocams’). Networks of phenocams have been set up (notably the PhenoCam Network; Richardson 2019, see also Wingate et al. 2015), which has enabled data to be centralised and harmonised. Image data are more complex than ground observation data. They have to be processed to extract an analysable phenological signal (e.g., critical dates in the development of the foliage). The development and public sharing of algorithms for processing phenocam images (e.g., R packages *phenopix* Filippa et al. 2016 and *xROI* Seyednasrollah et al. 2019) has increased the use and impact of these data. Several studies have been dedicated to the comparison of critical phenological dates observed from the ground and inferred from the analysis of phenocam datasets at a common site (e.g., Keenan et al. 2014; Soudani et al. 2021). They show a very good match between ground-observed and phenocam-inferred leaf-out dates at the community scale. More recently, we have shown by comparing ground observation and phenocam data that

the analysis of phenocam data also allows quantifying the intra-population variability of leaf-out (Delpierre et al. 2020). For this purpose, we subdivided the phenocam scene (i.e., region of interest, ROI, at the canopy scale) into several sub-ROIs (each targeting a particular tree) and analysed the data at this scale. The idea of analysing intra-canopy (i.e., intra-community) variability of leaf-out is not new and had previously appeared in site-scale studies (Ahrends et al. 2008; Richardson et al. 2009; Filippa et al. 2016). To our knowledge, it has not been deployed in the context of a regional study yet.

1.3 | Objectives

Here, we analysed phenocam data obtained over North American and European forests with the aim to investigate the determinants and ecological consequences of ICVLo in temperate deciduous forests. Specifically, we answered the following four questions:

1. Do variations in spring temperature influence similarly the date of leaf-out in North American and European temperate deciduous forests?
2. Is the higher species richness and/or phylogenetic diversity of North American forests associated with a higher ICVLo?
3. What are the environmental controls of ICVLo?
4. What are the ecological implications of ICVLo, in terms of light received and exposure to late frosts?

2 | Materials and Methods

2.1 | Study Sites

We analysed images taken by phenological cameras over 17 sites located in Europe (EUR, 8 sites) and Eastern North America (ENA, 9 sites) (Figure 1, Table 1). The sites were distributed

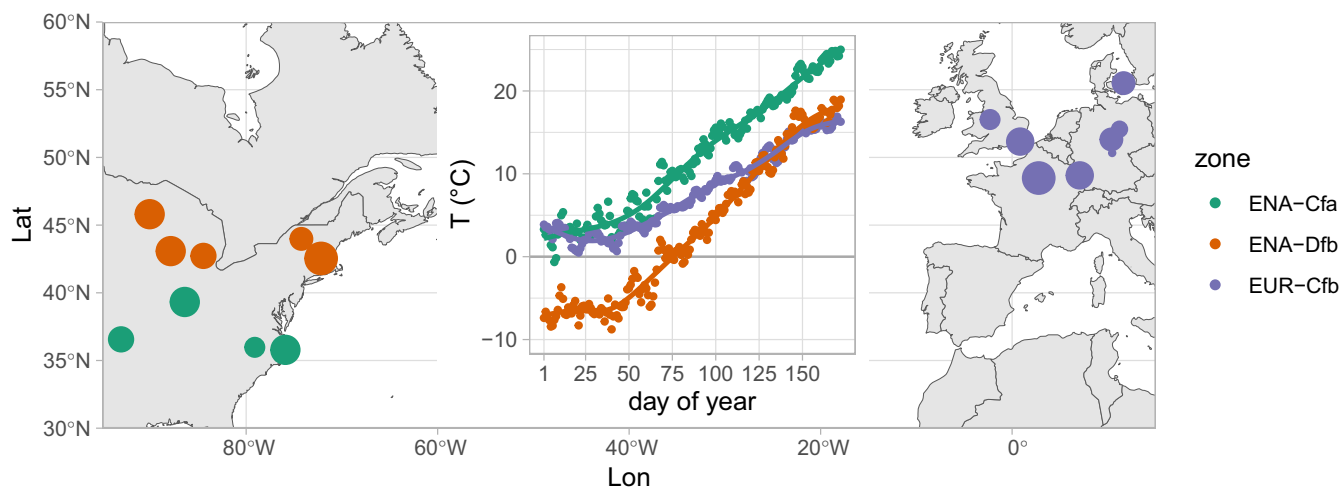


FIGURE 1 | Location of study sites. Colours indicate classification into Köppen climate zones. The size of points on the map scales with the number of years, ranging from 2 (smallest) to 10 (largest). The inset graph represents daily average air temperature climatologies (T , in °C) established over January to June; temperature data were binned according to day of year (DoY) and averaged across all study site-years of the corresponding climate zone. Climate zones are: Cfa = warm temperate with hot summer, Cfb = warm temperate with warm summer, Dfb = snow with warm summer.

TABLE 1 | Characteristics of study sites.

Site	Region	Lat (°N)	Lon (°E)	Köppen climate zone	Species number	Camera	Npix	Years	Leaf-out (DoY)	SD (days)
Alice-Holt	EUR	51.17	0.84	Cfb	2	Stardot	329	2011–2016, 2018, 2020	121.6/109.7/132.7	3.4/1.5/4.7
Barbeau (FR-Fon)	EUR	48.48	2.78	Cfb	2	Axis	153	2012–2022	105.6/96.7/115.7	4.1/1.6/9.9
Hainich (DE-Hai)	EUR	51.08	10.45	Cfb	3	Kodak, Canon	267	2011, 2017	124.0/114.7/133.3	3.9/1.4/6.3
Hohes Holz (DE-HoH)	EUR	52.08	11.21	Cfb	3	Stardot	426	2016–2018	118.7/110.6/125.5	5.7/1.4/10.4
Leinefelde (DE-Lnf)	EUR	51.33	10.37	Cfb	1	Stardot	246	2010, 2012–2016	118.5/106.1/128.2	1.5/0.3/2.6
Sorø (DK-Sor)	EUR	55.49	11.64	Cfb	1	Stardot	149	2014–2018	120.4/112.9/126.5	3.7/2.5/4.5
Hesse (FR-Hes)	EUR	48.67	7.06	Cfb	4	Stardot	285	2012–2018	112.5/101.8/120.8	2.8/1.0/7.7
Mill Haft	EUR	52.80	-2.30	Cfb	2	Stardot	302	2017–2020	116.8/110.8/125.5	4.6/3.1/7.5
Alligator River (US-NC4)	ENA	35.79	-75.90	Cfa	2	Stardot	164	2013–2020	101.2/91.6/107.9	2.4/1.4/4.9
Arbutus Lake	ENA	43.98	-74.23	Dfb	5	Stardot	241	2009–2014	133.8/127.1/139.7	3.6/1.6/5.1
Bull shoals	ENA	36.56	-93.07	Cfa	NA ^a	Stardot	105	2015–2020	105.7/101.3/118.7	2.2/1.4/3.7
Downer woods	ENA	43.08	-87.88	Dfb	4	Stardot	344	2013–2020	140.4/136.1/145.1	3.1/2.0/3.9
Duke HW (US-DK2)	ENA	35.98	-79.10	Cfa	5	Stardot	255	2014–2017	93.0/83.1/99.3	3.5/2.6/4.3
Harvard Forest (US-Hal)	ENA	42.53	-72.17	Dfb	4	Stardot	176	2009–2019	131.3/124.5/135.6	1.9/0.7/4.7
Morgan Monroe (US-MMS)	ENA	39.32	-86.41	Cfa	5	Stardot	239	2010–2017	105.5/86.6/117.8	4.7/2.7/7.9
Sanford	ENA	42.73	-84.46	Dfb	6	Stardot	322	2015–2020	121.8/109.1/125.7	2.4/0.7/3.8
Willow Creek (US-WCr)	ENA	45.80	-90.07	Dfb	4	Stardot	367	2015–2020	139.8/134.7/145.6	1.6/0.7/3.2

Note: Npix refers to the number of sub-ROIs analysed at each site. SD is the standard deviation of leaf-out dates. Columns leaf-out and SD contain the mean/minimum/maximum values observed at each site across the measuring time period (years). Köppen climate zones: Cfa = warm temperate with hot summer, Cfb = warm temperate with warm summer, Dfb = snow with warm summer. Stardot is for Stardot NetCam SC5MP, Axis is for Axis P1347, Kodak is for Kodak DC290, Canon is for Canon Powershot A700. The actual species names are displayed in Table S1.

^aSpecies number could not be determined at Bull shoals.

between 36°N and 56°N, and classified into Köppen–Geiger climate zones using the *kgc* package (Bryant et al. 2017), with zone names from Kottek et al. (2006). We selected these sites on the basis of the length of the image time series available and the general quality of the images (main criteria were: fixed field of view including a large proportion of forest cover and good image sharpness). The quality of the images was not always consistent between years for the same site, which led us to keep some years and discard others for a given site (Table 1). Analysed images were acquired from 2009 to 2022.

2.2 | Processing Phenocam Images

We obtained images from the phenocam dataset (Seyednasrollah et al. 2019) for 10 study sites (all the ENA sites plus Mill Haft). Images for the seven other sites were provided by the site PIs. For each site, we delineated a mask (ROI) to delimit the deciduous vegetation zone in the phenocam scene (i.e., excluding roads, buildings, the sky and evergreen trees), thanks to the R package *xROI* (Seyednasrollah, Milliman, and Richardson 2019). Since our aim was to work on ICVLo, we adopted a ‘pixel-based’ approach (Filippa et al. 2016) that has rarely been used to date for the analysis of phenocam images (but see Ahrends et al. 2008; Delpierre et al. 2020; Richardson et al. 2009). For this, we subdivided the ROI into sub-ROIs using a systematic hexagonal grid (Figure 2) with the R package *rgeos* (Bivand and Rundel 2023). The phenological sequence of each sub-ROI was analysed independently.

Using the sub-ROI approach in a previous work, we showed it was possible to retrieve intra-scene variability of leaf-out dates that were very close to the inter-tree variability of leaf-out observed from the ground (Delpierre et al. 2020). In our systematic grid approach, the mesh size was specifically chosen for each site according to the proximity and size of the tree crowns (Figure 2A). We chose mesh sizes that were slightly smaller than the average tree crown size observed on the grid, approximating one sub-ROI

to represent one tree. The idea here was to reduce the risk of an under-estimation of the ICVLo that would result from choosing too coarse mesh sizes (i.e., that would lead to confound canopy crowns), bearing in mind that the intra-crown variability of leaf-out is lower than the inter-crown variability (e.g., Smith 2018, their table A3.3). We conducted preliminary evaluation of the method on a subset of four sites, comparing the intra-scene variation of leaf-out obtained from the systematic grid versus a more detailed approach into which we identified sub-ROI at the scale of the tree (Supporting Information Notes S3). The error arising from the use of the systematic grid was of 0.36 days (see Figure S3.2), which yields a signal-to-noise ratio of 8.6 [calculated as the ratio of the average standard deviation (SD) of leaf-out, see next, to the error of 0.36 days]. We considered this value high enough to be confident in the quality of the analyses conducted on data obtained from the systematic grid approach.

2.3 | Retrieving Leaf-Out From the GCC Signal

In each sub-ROI, we determined the date of leaf-out from the analysis of the Green Chromatic Coordinate (GCC) time series (Keenan et al. 2014). GCC uses red (R), green (G) and blue (B) digital numbers to calculate the ratio of green within the image [$GCC = G/(R + G + B)$]. Specifically, we determined the ‘date of leaf-out’ of each sub-ROI with a threshold approach (Keenan et al. 2014), using 30% of the spring signal amplitude as a threshold (Figure 2B). We computed the lower bound of the signal amplitude as the 95th percentile of the GCC data obtained from day of year (DoY) 1 to 80 (blue line in Figure 2B). We computed the upper bound of the signal amplitude as the 98th percentile of the GCC data obtained over the whole year (green line in Figure 2B). After establishing the date of leaf-out for each sub-ROI, we first cross-checked the minimum and maximum dates of leaf-out against phenocam images. In eight site-years out of 106 site-years present in the dataset, the analysis of the GCC data produced too early or too late leaf-out dates in some sub-ROIs as compared to our visual inspections

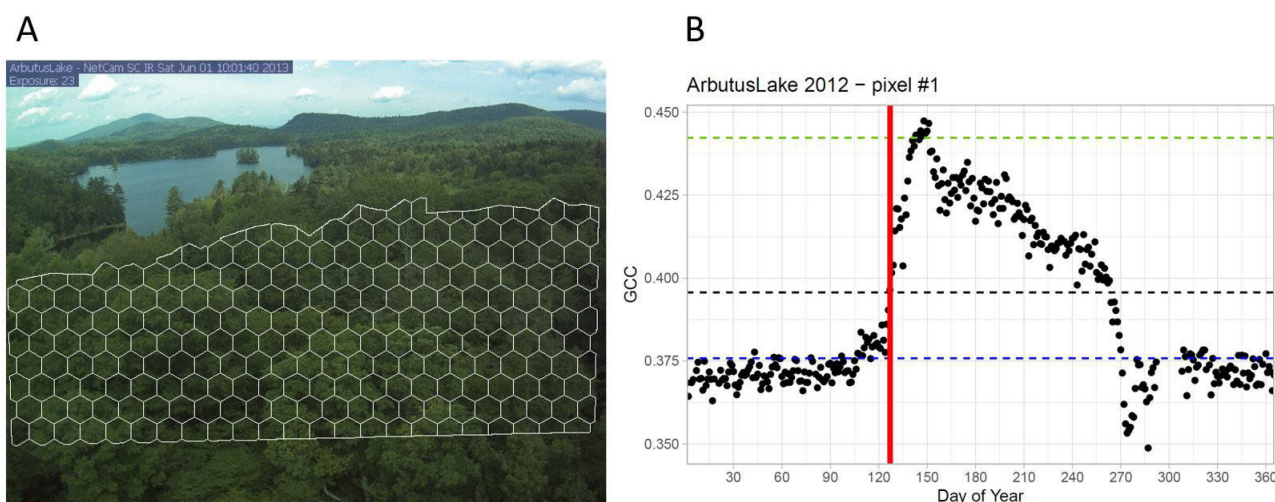


FIGURE 2 | Processing of the phenocam data. (A) Representation of a scene onto which a gridded region of interest (ROI) has been applied; (B) data extracted from one of the grid elements (i.e., one sub-ROI), where the blue horizontal line marks the minimum spring green chromatic coordinate (GCC) value, green horizontal line is the maximum GCC value considered and the black horizontal line represents 30% of the amplitude between the blue and green lines. Red vertical line is the leaf-out date determined for this particular grid element. Images and data are from Arbutus Lake site (NY, USA) in 2012.

of the phenocam images. We removed those outliers from the distributions of leaf-out dates determined at the sub-ROI scale. These outliers represented 3% of the sub-ROIs on average for the eight site-years considered. Then, we computed community-scale phenological metrics for each site-year in the dataset, namely the minimum, maximum and average leaf-out date (DoY), the leaf-out standard deviation (in days) and the amplitude (i.e., maximum–minimum, in days). In the following, we use the standard deviation of leaf-out (SD, in days) for quantifying ICVLo. Standard deviation is a measure of the average duration between each sub-ROI leaf-out date and the average date established over the whole community.

2.4 | Meteorological Data

We retrieved air temperature and radiation data of each site from nearby meteorological stations for ENA sites (except Bull shoals, for which we used data from the DAYMET database; Thornton et al. 2021) as well as for two European sites (Alice-Holt and Mill Haft), and from the ICOS community for the other European sites ('Warm Winter 2020 ecosystem eddy covariance flux product', <https://doi.org/10.18160/2G60-ZHAK>). In order to assess the influence of temperature conditions on ICVLo, we computed for each site-year the average temperature (Tmean, in°C) and the absolute minimum temperature occurring during the period of leaf-out. Preliminary analyses (Figure S4) identified that ICVLo was more strongly related to the minimum temperature measured during the period extending from the 5th to the 95th percentile of the sub-ROI distribution of leaf-out (hereafter Tmin, in °C).

In order to quantify how treewise light absorption was influenced by ICVLo, we compared the sum of radiation received by the community from (i) the leaf-out date of the earliest sub-ROI and (ii) the leaf-out date of the latest sub-ROI to October 1.

In order to compare the exposure of the earliest and latest trees in the community to late frosts, we quantified their respective 'safety margins'. Safety margin is defined as the duration (in days) between the leaf-out date of the earliest (or latest) sub-ROI and the occurrence of minimum temperatures below the critical threshold of -3°C (below which frost damage on emerging leaves is irreversible) during a period of leaf vulnerability lasting 25 days after leaf-out (Lin, Rathgeber, et al., 2024; see Figure S2 for a graphical depiction of safety margin calculation).

2.5 | Community Diversity Metrics

One of our objectives was to evaluate the influence of the community diversity on ICVLo, with the hypothesis that more diverse canopies would display higher ICVLo. For this, we considered two metrics for the diversity of the community. First, we considered the number of dominant tree species (*S_{pnum}*) that were visible in the site ROIs. Yet, the species number could be less informative than phylogenetically informed metric of the diversity, because leaf-out is a trait that is conserved in some clades (Panchen et al. 2014). Hence, we also considered

the *mean pairwise distance (MPD)* as a metric for community diversity. MPD is the mean phylogenetic distance (i.e., branch length) among all pairs of species within a community. Because all species composing a community do not have the same abundance in the analysed ROIs, we weighted the contribution of each species pair in MPD by the product of the individual species abundances (see Table S1). Calculations of MPD were done with the *picante* package (Kembel et al. 2010), using the tree phylogeny from Zanne et al. (2014). Since we could not identify the species identity and proportional contribution to ROI at Bull shoals, we included data from this site only in analyses that do not require these metrics (i.e., Figures 3, 4A,C,D, 5 and 6 in the main text and S5 in the supplementary material).

2.6 | Statistics

2.6.1 | Comparing Distributions Among Climate Zones

We used boxplots for graphical representations of the data. They display the median, first and third quartiles (box) and go up to the largest/lowest value, no further than 1.5 times the interquartile range (whiskers). Data beyond the end of the whiskers are plotted individually. When comparing distributions of data among climate zones, we applied non-parametric rank sum Wilcoxon tests.

2.6.2 | Statistical Models

In order to answer Question 1 (see Objectives), we tested the link between the average leaf-out date and spring temperature, taking into account a possible interaction of the climate zone (i.e., relation between average leaf-out date and temperature could differ among climate zones):

$$\text{DLO}_i \sim \text{MST}_i \times \text{CZ}_i \quad (1)$$

where DLO_i is the average date of leaf-out (DoY) for site-year i , MST is the mean spring (March–May) temperature ($^{\circ}\text{C}$) and CZ is the site climate zone.

Questions 2 and 3 were related to the influence of the community diversity and the environment on ICVLo. We first hypothesised that ICVLo, quantified as the SD of leaf-out dates, would be related to temperature and the date of leaf-out, perhaps differently across climate zones. Hence, we formulated a first model:

$$\text{SD}_i \sim (\text{Tmin}_i + \text{MinLO}_i) \times \text{CZ}_i \quad (2)$$

In order to test the hypothesis that more diverse communities display a higher SD, we further formulated two models:

$$\text{SD}_i \sim (\text{Tmin}_i + \text{MinLO}_i + \text{Spnum}_i) \times \text{CZ}_i \quad (3)$$

and

$$\text{SD}_i \sim (\text{Tmin}_i + \text{MinLO}_i + \text{MPD}_i) \times \text{CZ}_i \quad (4)$$

where SD_i is standard deviation of leaf-out (in days) for site-year i , T_{\min} is the minimum temperature measured during the period extending from the 5th to the 95th percentile of the sub-ROI distribution of leaf-out ($^{\circ}\text{C}$), MinLO is the date of leaf-out of the earliest sub-ROI, Spnum is the number of tree species contributing to the GCC signal on the phenocam ROIs and MPD is a measure of the phylogenetic distance computed over those species (see before).

We used generalised linear models (GLMs) with a gamma error distribution for fitting (Equations 2–4), because the SD data were non-Gaussian but followed a gamma distribution. The coefficients of a GLM relate to the mean by way of the assumed link function, which is the inverse function by default for a gamma GLM. Equations (2)–(4) include a number of terms, some of which may not be significant and hinder a proper estimation of the remaining, significant effects. In order to identify model structures including only significant terms, we used the *stepAIC* procedure in R. We compared the fitted models using the Akaike information criterion (AIC), considering that a difference of 2 AIC units points to a significant difference in model performance (Burnham and Anderson 2002). Data from the Bull shoals site could not be considered for the model fitting, because we missed information on the exact species number and identity and therefore could not estimate the *Spnum* and *MPD* variables there.

2.6.3 | Software Version

All analyses were conducted with the R software (R Core Team 2023). We used R version 3.6.2 for phenocam image processing and R version 4.2.2 for the data analysis, plotting and

statistical tests. Figures were plotted with the *ggplot2* package (Wickham 2016).

3 | Results and Discussion

3.1 | Spring Temperature Across Climate Zones

Temperatures during the first half of the year (January–June) differed markedly among the study climate zones (Figure 1, inset). Sites in the Dfb zone (snowy climate, with warm summer) of ENA experienced negative temperatures, averaging -7°C from DoY 1 to 50, followed by a steep increase with positive temperature reached from DoY 75 and $+5^{\circ}\text{C}$ reached on DoY 100. Temperatures remained positive from DoY 1 in the Cfa zone (warm temperate climate, with hot summer) of ENA and the Cfb zone (warm temperate climate, with warm summer) of EUR, with a steeper increase from DoY 50 in Cfa, as compared to Cfb. Temperatures reached $+8^{\circ}\text{C}$ and $+15^{\circ}\text{C}$ on DoY 100 in EUR-Cfb and ENA-Cfa respectively.

3.2 | Comparing the Leaf-Out Dates in ENA and EUR and Their Relationships to Temperature

Leaf-out dates averaged over the community spanned a larger range in ENA (from DoY 83, March 24 to DoY 146, May 26) than in EUR (from DoY 97, April 7 to DoY 133, May 13) (Figure 3). The distributions of leaf-out dates were significantly different among climate zones (pairwise Wilcoxon tests all returned $p < 0.001$, Figure 3A). Communities in ENA-Cfa leafed out on average on DoY 102 (April 12), 13 days earlier than EUR-Cfb (DoY 115, April 25) and 31 days earlier than ENA-Dfb (DoY 133, May 13).

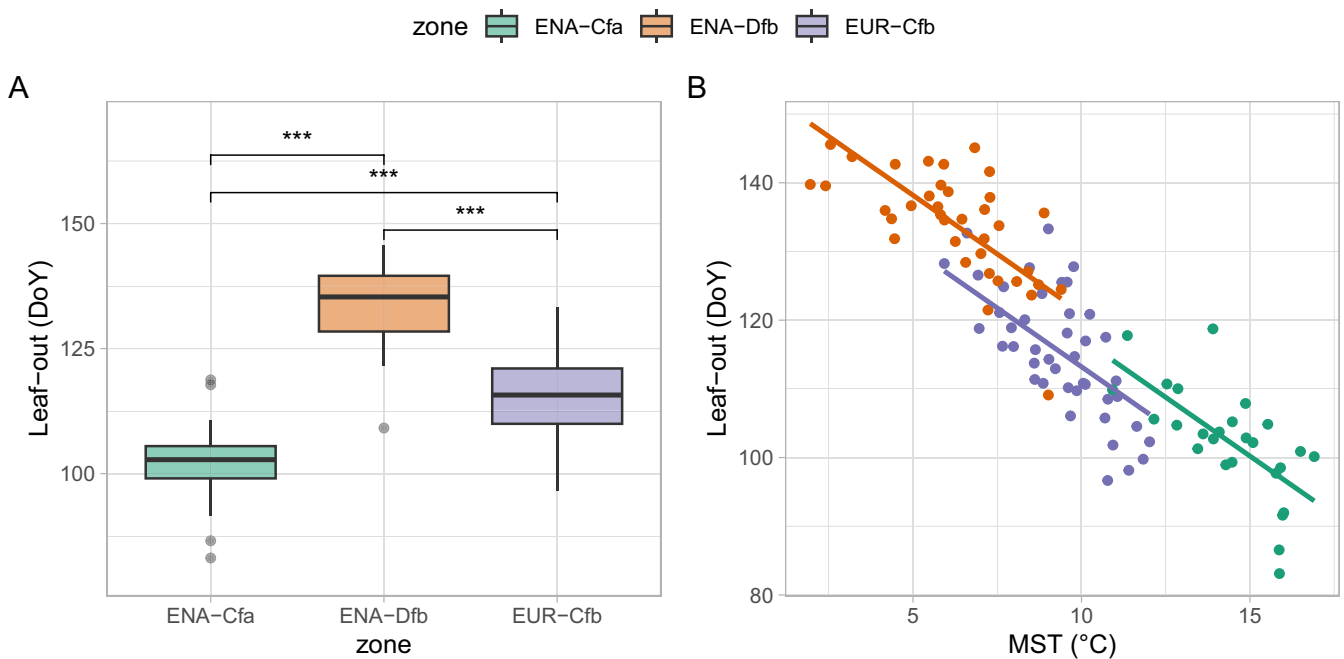


FIGURE 3 | Comparing leaf-out dates in EUR and ENA. Both plots display the average leaf-out dates (day of year, DoY) determined for each site-year at the scale of the community. The data are grouped by climate zone (colours). (A) Boxplots of the site-year average leaf-out; (B) relation of leaf-out with mean spring (March–May) temperature (MST). In (A), p values of Wilcoxon's tests are shown ($***p < 0.001$, $**p < 0.01$, $*p < 0.05$, $\cdot p < 0.10$, ns $p \geq 0.10$). In (B), linear regressions of leaf-out against MST are shown.

TABLE 2 | Output of a Linear Model Testing the Influence of Spring Temperature and Climate Zone on the Average Date of Leaf-Out. MST is mean spring (March–May) temperature, Zone identifies the climate zones.

Parameter	Estimate	SE	<i>t</i>	<i>p</i>
Intercept	151.54	5.57	27.2	< 10 ⁻¹⁵
MST	-3.42	0.38	-9.1	< 10 ⁻¹⁴
zone:ENA-Dfb ^a	3.75	3.47	1.1	0.28
zone:EUR-Cfb ^a	-4.11	2.46	-1.7	0.10

^aZone: ENA-Cfa set to zero.

The three climate zones displayed spring (March–May average) temperature ranges of about 6° (Figure 3B), with the warmest spring temperatures in ENA-Cfa and the lowest in ENA-Dfb (see also Figure 1 inset). Noticeably, the slopes of leaf-out to spring temperature were not significantly different among zones ($p < 0.14$, i.e., no interaction term was retained in Equation (1)), but the intercept were, albeit marginally (Figure 3B and Table 2: intercept of the relation was lower in EUR).

Intercontinental analyses of leaf-out dates have mostly been conducted through remote sensing studies (so-called ‘start of spring’ indices) (Piao et al. 2019; Jeong et al. 2011). They evidenced trends to earlier leaf-out with recent climate change, but to our knowledge did not compare the slopes (in days per degree) that quantify the sensitivity of leaf-out to air temperature. We show here that the slopes are virtually identical in ENA and EUR, despite peculiarities of the species compositions of the European and North American floras. The rate of change of leaf-out date per unit temperature change (-3.4 days per °C, Table 2), established here across continents, is in the range of those reported for European tree species during the ‘pre-season’ period (from -2.0 to -4.5 days per °C, Fu et al. 2015; Zohner, Mo, and Renner 2018). Other works have addressed the leaf-out of plants in botanical common gardens and showed that ENA species tend to leaf out later than EUR species when placed in the same climate conditions (e.g., Zohner et al. 2017, their Figure 3). Results from our regression analysis are in line with this. Indeed, for the same spring temperature, EUR forests leaf-out earlier than ENA forests (see Figure 3B, and the fact that the intercept of EUR-Cfb is lower than that of ENA-Cfa and ENA-Dfb, albeit marginally $p < 0.097$, Table 2).

3.3 | Comparing the Intra-Community Variability of Leaf-Out Dates in ENA and EUR, Its Dependence on Species Richness and Environmental Controls

The ICVLo dates were in the range of 0.3 to 10.4 days and averaged 3.1 days (3.2 days in ENA-Cfa, 2.4 days in ENA-Dfb and 3.6 days in EUR-Cfb, Figure 4A). The mean ranks between samples of SD were significantly different among climate zones (Kruskal–Wallis test $\chi^2 = 6.69$, $p < 0.04$), with ranks of the SD distribution being significantly lower in ENA-Dfb than in the two other zones (Figure 4A). We hypothesised that ICVLo would be larger than the intra-population variability (Figure S1). However, the average ICVLo of 3.1 days calculated over our data

(all zones grouped) was significantly lower (Wilcoxon rank sum test, $p < 0.003$) than the average standard deviation of leaf-out in tree populations that reached 4.0 days (data from Denéchére et al. 2021 consisting of 37 site-years of ground observations across 12 European tree populations). More precisely, the distribution of SD established at the community scale from phenocams in EUR was not different from the distribution of SD established at the population scale from the analysis of ground observations in European tree populations (Wilcoxon rank sum test, $p < 0.18$, Figure S5). However, the latter was significantly higher than the distribution of SD established from phenocams in ENA (Wilcoxon rank sum test, $p < 0.001$ for the comparison with ENA-Dfb and $p < 0.06$ for the comparison with ENA-Cfa, Figure S5).

Several studies have evaluated the relationship between leaf-out dates obtained from phenocams and those obtained from ground observation. These studies show that the leaf-out dates obtained from phenocams have an inter-annual amplitude very close to those obtained from ground observation (Delpierre et al. 2020; Keenan et al. 2014; Soudani et al. 2021). Hence, we hypothesise that the lower SD we observed at the scale of communities, as compared to SD observed at the scale of populations (Denéchére et al. 2021), arose from an under-sampling of the actual variability in our phenocam analysis. Since we observed no systematic under-estimation of SD due to our grid definition of sub-ROIs (Supporting Information Notes S3), we hypothesise this under-sampling could arise from the fact that phenocams point mostly to dominant overstorey trees, therefore overlooking inter-individual variations related to tree size (Gressler et al. 2015), developmental stage (Vitasse 2013) or micro-environmental conditions (Pérot et al. 2021) that are captured when conducting phenological observations from the ground.

The phenocam scenes included on average more species in ENA than in EUR (median number of species was 5 in ENA-Cfa, 4 in ENA-Dfb and 2 in EUR-Cfb, Figure S6A). This difference in species richness was also reflected in phylogenetic diversity, which was higher in ENA than in EUR (Figure S6B). There was no significant correlation between ICVLo and phylogenetic diversity, when considering all data together (Figure 4B, see Figure S4 for correlation analysis). However, ICVLo tended to increase with phylogenetic diversity in ENA-Dfb (rank correlation 0.38, $p < 0.03$) and ENA-Cfa (rank correlation 0.67, $p < 0.002$) (Figure 4B). In both EUR and ENA, SD decreased with warmer minimum temperatures during leaf-out (Figure 4C) and with the date of earliest leaf-out in the community (Figure 4D).

The model based on Equation (4), incorporating the influences of temperatures, date of leaf-out and a measure of the phylogenetic diversity of the community fitted the ICVLo data best (Table 3). The terms of the full model were generally coherent with the visual depiction from Figure 4, considering the model was fitted with an inverse link function (see Methods). For instance, the coefficient estimates for variables Tmin and MinLO were positive in the model (Table 4), coherent with the negative correlation of SD with those variables (Figure 4C,D). The interaction term Tmin*EUR-Cfb was positive, indicating that the response of SD to temperature in EUR-Cfb was more pronounced (i.e., with a steeper negative slope) than in

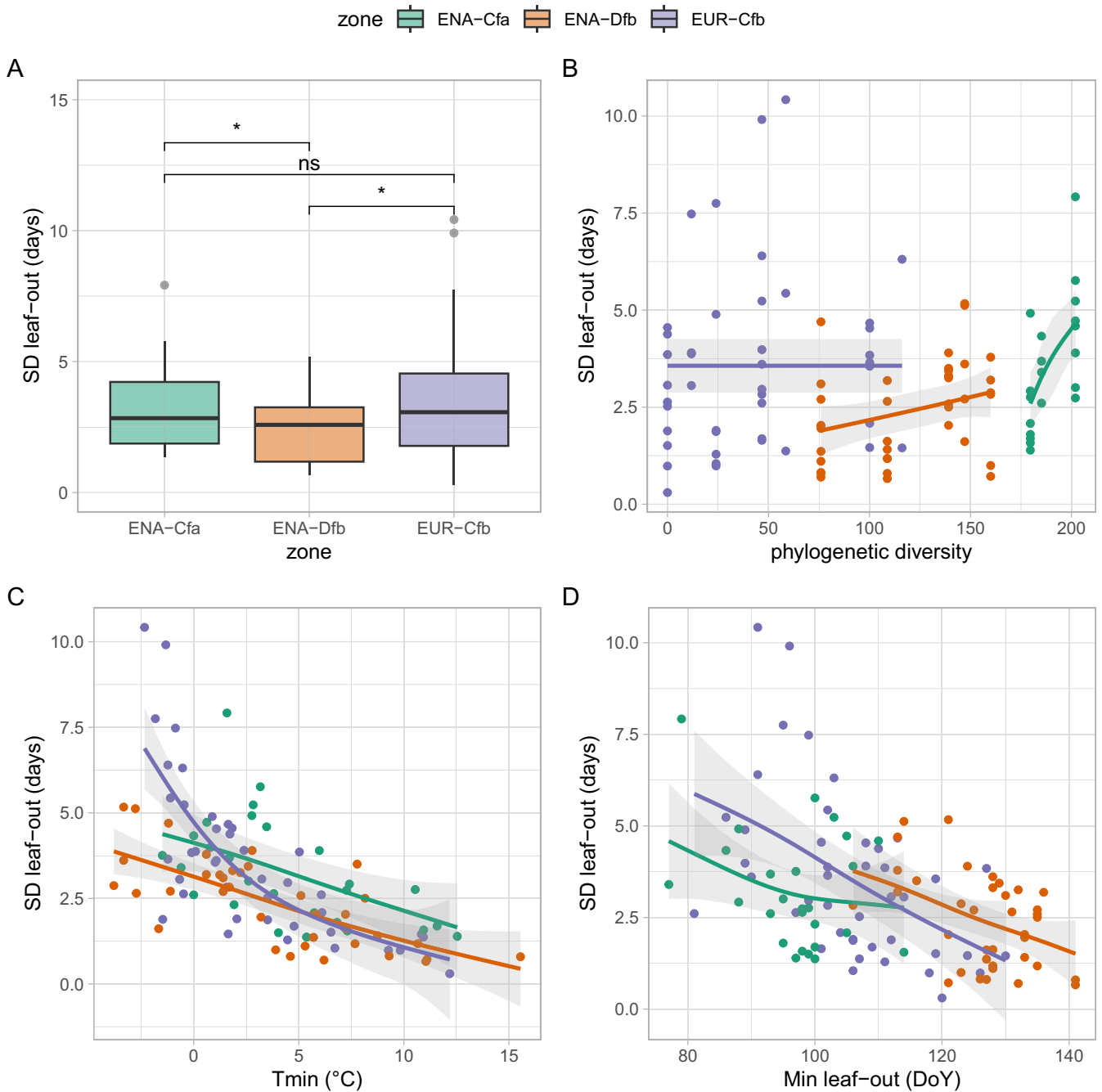


FIGURE 4 | The intra-community variability of leaf-out dates in EUR and ENA. All plots display the standard deviation (SD, in days) of leaf-out dates determined for each site-year at the scale of the community. (A) Distributions of the SDs of leaf-out in EUR and ENA; relation of SD with: (B) the phylogenetic diversity of communities, quantified as mean pairwise distance among species (see text); (C) the minimum temperature recorded over percentiles 5 to 95 of the leaf-out period; (D) the minimum date of leaf-out observed on the considered site-year. In (A), *p* values of Wilcoxon's tests are shown (***p* < 0.001, ***p* < 0.01, **p* < 0.05, ·*p* < 0.10, ns *p* ≥ 0.10). In (B–D), the lines display fits of generalised additive models (GAMs), used here for visualisation purposes. In (B), data from Bull shoals were omitted (see text).

ENA-Cfa and ENA-Dfb (see also Figure 4C). One hypothesis for this pattern is that the (intra-community) distribution of the sum of temperatures required to reach budburst is wider in EUR than in ENA, despite a lower phylogenetic diversity. This wider distribution could stem from a lower selection pressure of minimum temperatures in EUR, as compared to ENA where the steeper spring temperature increase (Figure 1) may prevent the survival of anomalously early trees, as compared

to the community average. The interaction terms MPD×EUR-Cfb and MPD×ENA-Dfb were both positive, indicating that the response to MPD was weaker there than in ENA-Cfa (see Figure 4B).

The correlation of ICVLo with minimum temperatures occurring during the leaf-out period (Figure 4C) mirrors earlier results obtained at the scale of tree populations (Denéchére et al. 2021).

Warmer springs have been shown to hasten the speed of leaf-out across scales, from the scale of the bud (Basler and Körner 2014) to the individual tree crown (Denéchère et al. 2021), to the population (Denéchère et al. 2021). Here, we show that this result extends to the scale of the community. Recently, Lin, Berveiller, et al. (2024) developed a model simulating the progress of leaf-out at the scale of a tree population. In this model, each individual tree has a particular sum of forcing temperatures to reach for leaf-out to occur. In line with our results, the model predicts a longer period of time from the first to last tree to leaf-out (hence extended intra-specific variability) during cooler springs (see also Figure S1 of Denéchère et al. 2021).

A study conducted at the scale of Germany showed that warmer springs resulted in a 'loss of phenological synchrony' (i.e., higher variability of leaf-out) among populations of European Beech trees (Zohner, Mo, and Renner 2018). Our results could appear to contradict this work, because we found a negative link between ICVLo and temperature during leaf-out (i.e., warmer temperatures during leaf-out are associated with smaller ICVLo, that is a higher phenological synchrony in the communities). This contradiction disappears once we take into account the fact that

these two studies do not consider the effect of temperatures in the same time window. We related ICVLo to the temperature conditions occurring during the period of leaf-out (Figure 4C), while Zohner, Mo, and Renner (2018) considered temperature conditions occurring during the 60 days preceding the average date of leaf-out. Similar to Zohner, Mo, and Renner (2018); (their Figure 1E), we found that early leaf-out (caused by a high 'pre-season' temperature) was associated with a higher variability of leaf-out (Figure 4D). However, the influence of the date of leaf-out on ICVLo was of second order, as compared to the influence of temperature conditions during leaf-out (i.e., partial correlations of SD with temperature, controlling for leaf-out date, were stronger than partial correlations of SD with date, controlling for temperature, see Table 5).

3.4 | Ecological Implications of the Intra-Community Variability of Leaf-Out

The date of leaf-out marks the start of the seasonal acquisition of carbon and loss of water through transpiration, as well as the start of the frost vulnerability window of new leaves. An increase in the ICVLo was associated, as expected, with an increase in the intra-community variability of radiation received, with no distinction among climate zones (Figure 5A). More specifically, individual trees which leaf-out first in the community received on average 8% more radiation (from 7% in ENA-Cfa to 10% in ENA-Dfb) from leaf-out to September than the last trees leafing-out (remembering we focused here on the dominant overstory trees) (Figure 6A). Under the naive hypothesis that photosynthesis scales with incoming radiation, as in a simple light-use efficiency (LUE) model (Baldocchi and Peñuelas 2019), and that NPP (net primary productivity or biomass productivity) is proportional to GPP (gross primary productivity, the gross amount of carbon fixed by photosynthesis) (Collalti and Prentice 2019), and ignoring intraspecific and leaf age variation in LUE, this would straightforwardly translate in a 8% difference in tree growth. This potential 8% difference

TABLE 3 | Comparing models fitted to the ICVLo data.

Model	Predictors	df	AIC	R ²
Equation 2	(Tmin + MinLO)×CZ	93	302	0.65
Equation 3	(Tmin + MinLO + Spnum)×CZ	88	302	0.66
Equation 4	(Tmin + MinLO + MPD)×CZ	90	297	0.71

Note: *df* is the number of degrees of freedom, obtained after model structure simplification by the *stepAIC* procedure. *AIC* is the Akaike information criterion. See text for the description of models.

TABLE 4 | Summary of the Best generalised linear model fit to the SD data.

Parameter	Estimate	SE	<i>t</i>	<i>p</i>
Intercept	1.30	0.47	2.77	0.006
Tmin	0.015	0.008	1.94	0.06
MinLO	0.0035	0.0012	2.91	0.005
MPD	-0.007	0.002	-3.04	0.003
EUR-Cfb ^a	-1.41	0.48	-2.95	0.004
ENA-Dfb ^a	-1.32	0.50	-2.63	0.01
Tmin×EUR-Cfb ^b	0.029	0.01	3.07	0.003
Tmin×ENA-Dfb ^b	0.017	0.01	1.72	0.09
MPD×EUR-Cfb ^c	0.007	0.002	2.84	0.005
MPD×ENA-Dfb ^c	0.007	0.003	2.60	0.01

Note: The model (Equation 4) was fitted with a gamma error distribution, using an inverse link function. Only terms of the models retained by the *stepAIC* procedure are displayed here. *SE* is the standard error of the parameter, *MinLO* is the minimum leaf-out date, *Spnum* is the species number, *MPD* is a measure of the phylogenetic diversity in the community. See text for details.

^aENA-Cfa set to zero.

^bTmin×ENA-Cfa set to zero.

^cMPD×ENA-Cfa set to zero.

is much smaller than the variability observed in basal area increment of tree growth we compute, for example, at the Barbeau (FR-Fon) forest (Table 1) for which we could access individual tree growth data (coefficient of variation of tree basal area increment, normalised by crown area was 35% among dominant trees). Along with other evidence (e.g., the fact that phenological rank in tree populations are not systematically correlated with growth, Delpierre et al. 2017), this points to a second-order influence of leaf phenology in determining the inter-individual growth of trees (see also Čufar et al. 2015; Charlet de Sauvage et al. 2022).

The probability of exposure to frost damage was not related to the SD of leaf-out (Figure 5B), in spite of the dependence of the SD of leaf-out to low temperatures (e.g., Figure 4C). Indeed, frost damages typically occur at temperatures below -3°C which may (in which case the safety margin to frost will be negative) or may not (in which case the safety margin to frost will be positive) happen during a cold spring with high SD of leaf-out. Remarkably, the safety margin against exposure to frost

was significantly smaller in ENA than in EUR (Figure 6B). As expected considering the trend to increasing temperatures in spring, early sub-ROIs had a smaller safety margin than late sub-ROIs, whatever the climate zone (Figure 6B, average safety margins in the 'earliest' sub-ROI were smaller than in the 'latest' sub-ROI). In EUR, we detected 1 site-year (i.e., 2% of the EUR data, Table 6) for which the earliest sub-ROI was exposed to a frost below -3°C . In ENA, this rose to 4 site-years (6% of the ENA data), belonging to two sites, both located in the cooler ENA-Dfb zone (Figure 1 inset). This result is consistent with calculations of a higher probability of frost exposure for North American, as compared to European species (Zohner et al. 2020), and suggests that North American temperate forests, indeed, experience late frosts more frequently than European forests. Not only the frequency, but also the extent of exposure to frost of ENA versus EUR forests differed in our dataset. When late frost strikes ENA forests, it could affect a large proportion of the community (Table 6).

TABLE 5 | Partial correlation of SD with temperature and leaf-out date.

	Partial r	p
$\rho(SD, T_{min} AveLO)$	-0.63	<0.001
$\rho(SD, AveLO T_{min})$	-0.21	<0.03
$\rho(SD, T_{min} MinLO)$	-0.60	<0.001
$\rho(SD, MinLO T_{min})$	-0.42	<0.001

Note: *AveLO* is the average leaf-out date, *MinLO* is the minimum leaf-out date. For example, $\rho(SD, T_{min} | AveLO)$ is the partial correlation of SD with T_{min} , controlling for *AveLO*.

4 | Conclusions and Perspectives

We were able to characterise the ICVLo dates through the analysis of images acquired automatically by phenological cameras. This methodological achievement is a promising step in the process of characterising the current and past variability of ecological traits in tree communities (e.g., the grid-based analysis of images could be applied to other ecological traits such as detecting variations in the health status and differential attacks by herbivores) with implications on the forest biocenosis (e.g., the timing of leaf emergence determines the availability of food for many herbivorous insect species). It complements other attempts to characterise the variability of phenology at the scale

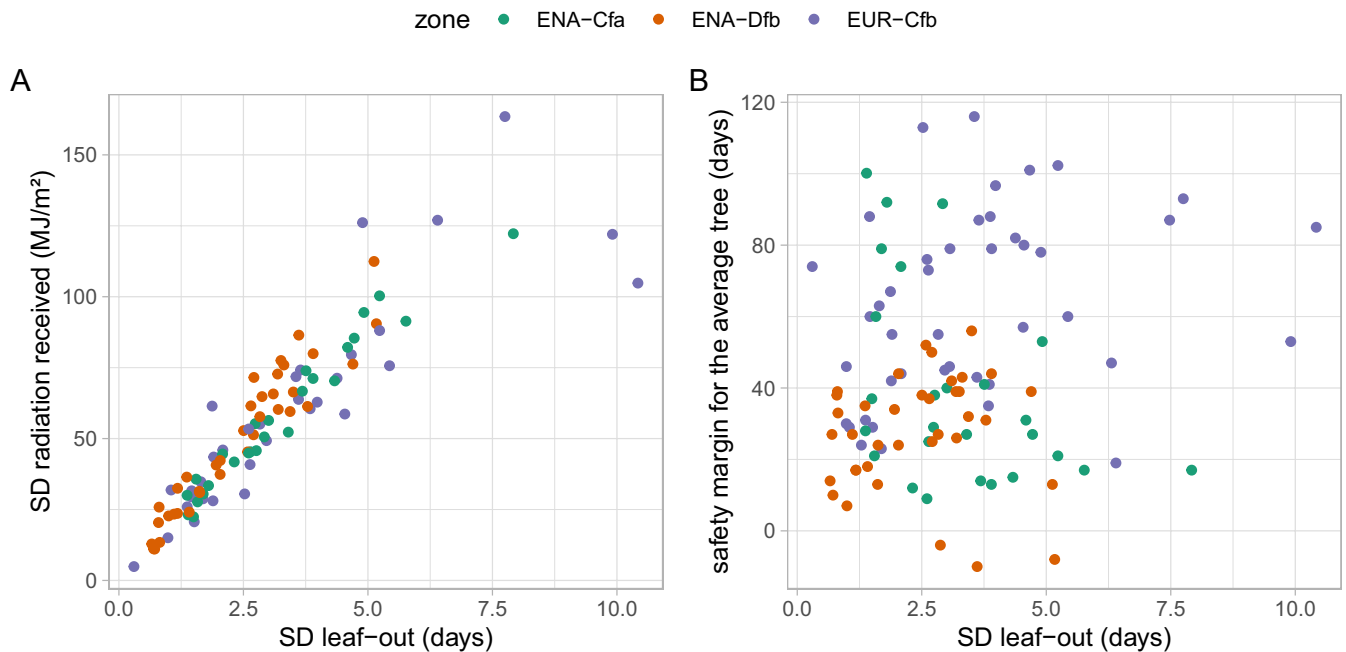


FIGURE 5 | Functional impacts of the intra-community variability of leaf-out at the community scale. (A) The relation between the intra-community variability of the amount of radiation received over the leaf-out period to October 1 and the SD of leaf-out; (B) the relation between the frost safety margin of the 'average tree' (i.e., individual tree leafing-out on the average date of the population for a given site-year) and the SD of leaf-out.

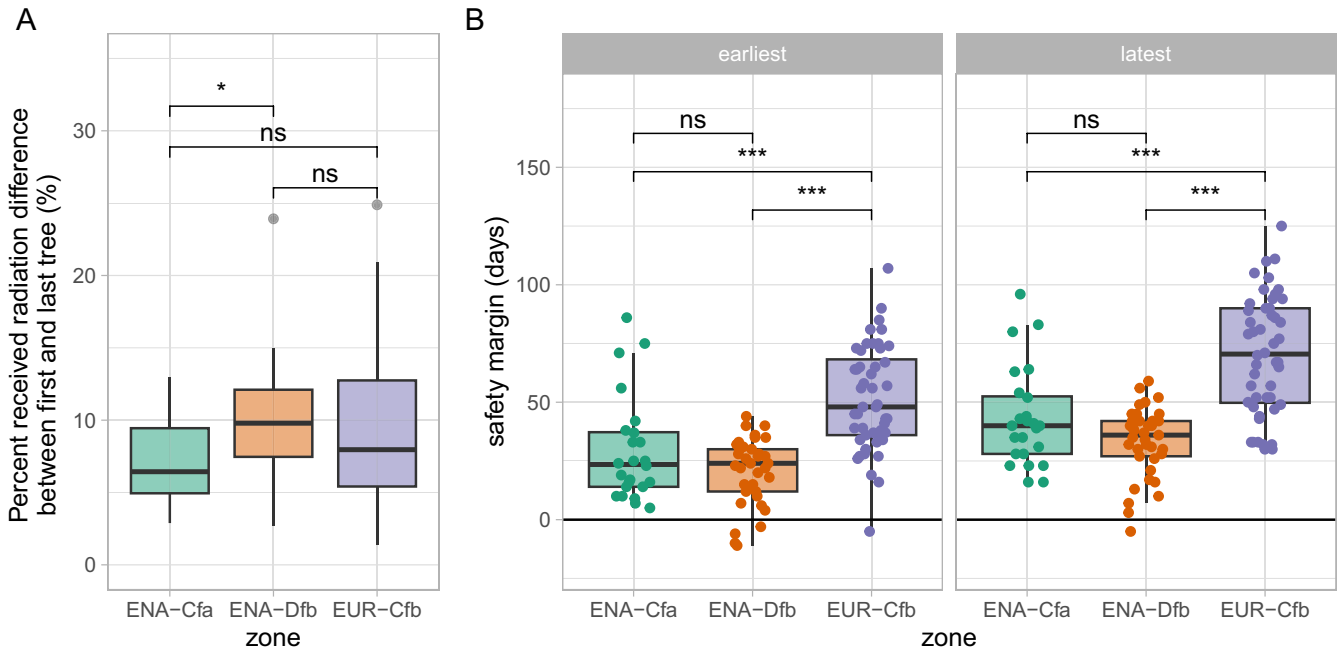


FIGURE 6 | Functional impacts of the intra-community variability of leaf-out at the individual scale. (A) The relative amount of excess radiation received by the earliest compared to the latest sub-ROI in the community; (B) the safety margin (in days) of the earliest and latest sub-ROI (two panels), as regards exposure of emerging leaves to temperatures lower than -3°C . In panel (B), data points are displayed over their respective boxplots in order to highlight the spread and identify clearly cases with a negative safety margin.

TABLE 6 | Percent of the community affected by late spring frost.

Zone	Site	Year	Percent frost (%)
ENA-Dfb	Arbutus Lake	2009	96
ENA-Dfb	Arbutus Lake	2010	73
ENA-Dfb	Arbutus Lake	2013	1
ENA-Dfb	Sanford	2020	89
EUR-Cfb	Barbeau	2021	1

Note: We report here the percentage of sub-ROIs that were in the 25-day vulnerability window following leaf-out when late frost ($T_{\text{min}} < -3^{\circ}\text{C}$) occurred.

of a landscape, using unmanned aerial vehicles (Klosterman et al. 2018; Berra, Gaulton, and Barr 2019) or satellite data (Moon et al. 2022). We have analysed data from 17 sites in EUR and ENA, totalling 106 site-years. As phenocam data accumulate, it will be possible to assess the genericity of our results by including more site-years on the same sites, as well as new sites, possibly on other continents (e.g., Asia via the Pheno-Eye network).

We found ample ICVLo at all study sites. The ICVLo was comparable in ENA and EUR, despite ENA forest canopies being more species-rich and phylogenetically diverse, pointing to a stronger environmental than biotic control of ICVLo. We highlight here that our approach based on phenocams focuses on dominant trees and not the whole forest tree community (i.e., it does not consider trees from the understory). In order to assess the influence of the diversity of the whole tree community on ICVLo, it would be necessary to monitor tagged individual trees visually from the ground. The ecological consequences of ICVLo are at least twofold: (1) on average, trees that leaf-out the earliest in a

community were exposed to about 8% more radiation from leaf-out to September than the latest trees, (2) those early trees have a lower safety margin regarding exposure to late frost and the safety margin was smaller in ENA as compared to EUR. Further ecological consequences of ICVLo remain to be explored, for example the impact of ICVLo on soil water content in a context of drier environmental conditions. The approaches developed in this work could also be extended to the analysis of the intra-community variability in leaf senescence, which is even greater than ICVLo (Delpierre et al. 2017) and whose determinants are probably more complex.

Acknowledgements

We thank our many collaborators, including site PIs and technicians, for their efforts in support of this study, and the PhenoCam network. In particular, we thank PIs from the European Integrated Carbon Observation System (ICOS) for providing the meteorological data and site information. We thank Sara DiBacco Childs (Duke Forest Executive Director) and Blake Tedder (Assistant Director of Engagement, Duke University) for their contribution. We thank Dr. Lenoir and four anonymous referees for their comments and suggestions, which helped improving the original manuscript. N.D. acknowledges funding from ANR (TAW-tree project, grant #ANR-23-CE01-0008-01). The development of PhenoCam has been funded by the Northeastern States Research Cooperative, NSF's Macrosystems Biology programme (awards EF-1065029 and EF-1702697) and DOE's Regional and Global Climate Modelling programme (award DE-SC0016011). J.L. was funded by the China Scholarship Council (grant #202008330320). A.K. and F.K. were funded by the German Federal Ministry of Education and Research (BMBF) as part of ICOS, by the Deutsche Forschungsgemeinschaft (INST 186/1118-1 FUGG) and by the Ministry of Lower-Saxony for Science and Culture [DigitalForst: Niedersächsisches Vorab (ZN 3679)]. M.W. acknowledges funding from the UK Forestry commission. A.N. acknowledges funding from DOE Ameriflux Network Management

Project, DOENICCR 08-SC-NICCR-1072, DOE-TES 11-DE-SC-0006700, USDA Forest Service Eastern Forest Environmental Threat Assessment Center 08-JV-11330147-038 and 13-JV-11330110-081. J.-C.D. acknowledges funding from DOE DE-SC0023309, PHYdraCC #ANR-21-CE02-0033-02. J.W.M. acknowledges funding from DOE DE-AC02-05CH11231, NSF LTER DEB-1832210. S.O.D. acknowledges funding from NIFA (award #2021-67034-35129). K.D. acknowledges funding from the National Science Foundation DEB-2044818 and USDA Hatch Project #M1CL02716. K.M.H. and G.C. were funded by the JABBS Foundation and the University of Birmingham. A.R.D. acknowledges funding from DOE Ameriflux Network Management Project award to ChEAS core site cluster.

Conflicts of Interest

The authors declare no conflicts of interest.

Data Availability Statement

Image data from the PhenoCam network (all ENA sites plus Mill Haft) are available at <https://phenocam.nau.edu/webcam/>. Phenocam data from the European sites are available on Dryad (<https://datadryad.org/stash/share/4v4ykf1EsLOrmB8tC2EIWIX2XdK8R640-ZF0M6g2Fus>). Code developed for phenocam image processing is available on Zenodo (with DOI [10.5281/zenodo.11387685](https://doi.org/10.5281/zenodo.11387685)). Code used for data analysis is available on Zenodo (with DOI [10.5281/zenodo.11395154](https://doi.org/10.5281/zenodo.11395154)).

References

- Ahrends, H. E., R. Bräugger, R. Stöckli, et al. 2008. "Quantitative Phenological Observations of a Mixed Beech Forest in Northern Switzerland With Digital Photography." *Journal of Geophysical Research: Biogeosciences* 113, no. 4: 0650.
- Alberto, F., L. Bouffier, J. M. Louvet, J. B. Lamy, S. Delzon, and A. Kremer. 2011. "Adaptive Responses for Seed and Leaf Phenology in Natural Populations of Sessile Oak Along an Altitudinal Gradient." *Journal of Evolutionary Biology* 24, no. 7: 1442–1454.
- Arend, M., A. Geßler, and M. Schaub. 2016. "The Influence of the Soil on Spring and Autumn Phenology in European Beech." *Tree Physiology* 36, no. 1: 78–85.
- Baldocchi, D., and J. Peñuelas. 2019. "The Physics and Ecology of Mining Carbon Dioxide From the Atmosphere by Ecosystems." *Global Change Biology* 25, no. 4: 1191–1197.
- Barr, A. G., T. A. Black, E. H. Hogg, et al. 2007. "Climatic Controls on the Carbon and Water Balances of a Boreal Aspen Forest, 1994–2003." *Global Change Biology* 13, no. 3: 561–576.
- Basler, D., and C. Körner. 2014. "Photoperiod and Temperature Responses of Bud Swelling and Bud Burst in Four Temperate Forest Tree Species." *Tree Physiology* 34, no. 4: 377–388.
- Berra, E. F., R. Gaulton, and S. Barr. 2019. "Assessing Spring Phenology of a Temperate Woodland: A Multiscale Comparison of Ground, Unmanned Aerial Vehicle and Landsat Satellite Observations." *Remote Sensing of Environment* 223: 229–242.
- Betancourt, J. L., M. D. Schwartz, D. D. Breshears, et al. 2007. "Evolving Plans for the USA National Phenology Network." *Eos, Transactions of the American Geophysical Union* 88: 211.
- Bivand, R., and C. Rundel. 2023. "rgeos: Interface to Geometry Engine—Open Source ('GEOS')." <https://github.com/rgeos/rgeos>.
- Bontemps, A., F. Lefèvre, H. Davi, and S. Oddou-Muratorio. 2015. "In Situ Marker-Based Assessment of Leaf Trait Evolutionary Potential in a Marginal European Beech Population." *Journal of Evolutionary Biology* 29, no. 3: 514–527.
- Bryant, C., Wheeler, N., Rubel, F., and French, R. 2017. kgc: Koeppen-Geiger Climatic Zones. R Package Version 1.0.0.2.
- Burnham, K., and D. Anderson. 2002. *Model Selection and Multimodel Inference: A Practical Information-Theoretic Approach*. New York, USA: Springer Verlag.
- Charlet de Sauvage, J., Y. Vitasse, M. Meier, S. Delzon, and C. Bigler. 2022. "Temperature Rather Than Individual Growing Period Length Determines Radial Growth of Sessile Oak in the Pyrenees." *Agricultural and Forest Meteorology* 317: 108885.
- Cole, E. F., and B. C. Sheldon. 2017. "The Shifting Phenological Landscape: Within- and Between-Species Variation in Leaf Emergence in a Mixed-Deciduous Woodland." *Ecology and Evolution* 7, no. 4: 1135–1147.
- Collalti, A., and I. C. Prentice. 2019. "Is NPP Proportional to GPP? Waring's Hypothesis 20 Years on." *Tree Physiology* 39, no. 8: 1473–1483.
- Čufar, K., M. De Luis, P. Prislan, et al. 2015. "Do Variations in Leaf Phenology Affect Radial Growth Variations in *Fagus sylvatica*?" *International Journal of Biometeorology* 59, no. 8: 1127–1132.
- Dantec, C. F., H. Ducasse, X. Capdevielle, O. Fabreguettes, S. Delzon, and M. L. Desprez-Loustau. 2015. "Escape of Spring Frost and Disease Through Phenological Variations in Oak Populations Along Elevation Gradients." *Journal of Ecology* 103: 1044–1056.
- Davies, T. J., E. M. Wolkovich, N. J. Kraft, et al. 2013. "Phylogenetic Conservatism in Plant Phenology." *Journal of Ecology* 101, no. 6: 1520–1530.
- Delpierre, N., J. Guillemot, E. Dufrêne, S. Cecchini, and M. Nicolas. 2017. "Tree Phenological Ranks Repeat From Year to Year and Correlate With Growth in Temperate Deciduous Forests." *Agricultural and Forest Meteorology* 234–235: 1–10.
- Delpierre, N., K. Soudani, D. Berveiller, E. Dufrêne, G. Hmimina, and G. Vincent. 2020. "'Green Pointillism': Detecting the Within-Population Variability of Budburst in Temperate Deciduous Trees With Phenological Cameras." *International Journal of Biometeorology* 64, no. 4: 663–670.
- Delpierre, N., K. Soudani, C. François, et al. 2009. "Exceptional Carbon Uptake in European Forests During the Warm Spring of 2007: A Data-Model Analysis." *Global Change Biology* 15, no. 6: 1455–1474.
- Delpierre, N., Y. Vitasse, I. Chuine, et al. 2016. "Temperate and Boreal Forest Tree Phenology: From Organ-Scale Processes to Terrestrial Ecosystem Models." *Annals of Forest Science* 73, no. 1: 5–25.
- Denéchère, R., N. Delpierre, E. N. Apostol, et al. 2021. "The Within-Population Variability of Leaf Spring and Autumn Phenology is Influenced by Temperature in Temperate Deciduous Trees." *International Journal of Biometeorology* 65, no. 3: 369–379.
- Donnelly, A., R. Yu, A. Caffarra, et al. 2017. "Interspecific and Interannual Variation in the Duration of Spring Phenophases in a Northern Mixed Forest." *Agricultural and Forest Meteorology* 243: 55–67.
- Eiserhardt, W. L., F. Borchsenius, C. M. Plum, A. Ordóñez, and J. C. Svenning. 2015. "Climate-Driven Extinctions Shape the Phylogenetic Structure of Temperate Tree Floras." *Ecology Letters* 18, no. 3: 263–272.
- Filippa, G., E. Cremonese, M. Migliavacca, et al. 2016. "Phenopix: A R Package for Image-Based Vegetation Phenology." *Agricultural and Forest Meteorology* 220: 141–150.
- Fu, Y. H., H. Zhao, S. Piao, et al. 2015. "Declining Global Warming Effects on the Phenology of Spring Leaf Unfolding." *Nature* 526, no. 7571: 104–107.
- Gressler, E., S. Jochner, R. M. Capdevielle-vargas, L. Patricia, C. Morellato, and A. Menzel. 2015. "Vertical Variation in Autumn Leaf Phenology of *Fagus sylvatica* L. in Southern Germany." *Agricultural and Forest Meteorology* 201: 176–186.
- Jeong, S. J., C. H. Ho, H. J. Gim, and M. E. Brown. 2011. "Phenology Shifts at Start vs. End of Growing Season in Temperate Vegetation Over

- the Northern Hemisphere for the Period 1982-2008." *Global Change Biology* 17, no. 7: 2385–2399.
- Keenan, T. F., B. Darby, E. Felts, et al. 2014. "Tracking Forest Phenology and Seasonal Physiology Using Digital Repeat Photography: A Critical Assessment." *Ecological Applications* 24, no. 6: 1478–1489.
- Kembel, S. W., P. D. Cowan, M. R. Helmus, et al. 2010. "Picante: R Tools for Integrating Phylogenies and Ecology." *Bioinformatics* 26, no. 11: 1463–1464.
- Klosterman, S., E. Melaas, J. Wang, et al. 2018. "Fine-Scale Perspectives on Landscape Phenology From Unmanned Aerial Vehicle (UAV) Photography." *Agricultural and Forest Meteorology* 248: 397–407.
- Kottek, M., J. Grieser, C. Beck, B. Rudolf, and F. Rubel. 2006. "World Map of the Köppen-Geiger Climate Classification Updated." *Meteorologische Zeitschrift* 15, no. 3: 259–263.
- Latham, R. E., and R. E. Ricklefs. 1993. *Continental Comparisons of Temperate-Zone Tree Species Diversity*, 294–317. Chicago, IL: The University of Chicago press.
- Lechowicz, M. J. 1984. "Why Do Temperate Deciduous Trees Leaf Out at Different Times? Adaptation and Ecology of Forest Communities." *American Naturalist* 124: 821–842.
- Liang, J., J. G. Gamarra, N. Picard, et al. 2022. "Co-Limitation Towards Lower Latitudes Shapes Global Forest Diversity Gradients." *Nature Ecology & Evolution* 6, no. 10: 1423–1437.
- Lin, J., D. Berveiller, C. François, et al. 2024. "A Model of the Within-Population Variability of Budburst in Forest Trees." *Geoscientific Model Development* 17, no. 2: 865–879.
- Lin, J., C. B. K. Rathgeber, and N. Delpierre. 2024. "Decreasing Frequency and Extent of Frost Damages in European Oaks Over 1961–2021. In prep."
- Moon, M., A. D. Richardson, T. Milliman, and M. A. Friedl. 2022. "A High Spatial Resolution Land Surface Phenology Dataset for AmeriFlux and NEON Sites." *Scientific Data* 9, no. 1: 448.
- Panchen, Z. A., R. B. Primack, B. Nordt, et al. 2014. "Leaf Out Times of Temperate Woody Plants Are Related to Phylogeny, Deciduousness, Growth Habit and Wood Anatomy." *New Phytologist* 203, no. 4: 1208–1219.
- Pérot, T., P. Balandier, C. Couteau, et al. 2021. "Budburst Date of *Quercus petraea* is Delayed in Mixed Stands With *Pinus sylvestris*." *Agricultural and Forest Meteorology* 300: 108326.
- Piao, S., Q. Liu, A. Chen, et al. 2019. "Plant Phenology and Global Climate Change: Current Progresses and Challenges." *Global Change Biology* 25, no. 6: 1922–1940.
- R Core Team. 2023. *R: A Language and Environment for Statistical Computing*. Vienna: Austria.
- Richardson, A. D. 2019. "Tracking Seasonal Rhythms of Plants in Diverse Ecosystems With Digital Camera Imagery." *New Phytologist* 222, no. 4: 1742–1750.
- Richardson, A. D., T. A. Black, P. Ciais, et al. 2010. "Influence of Spring and Autumn Phenological Transitions on Forest Ecosystem Productivity." *Philosophical Transactions of the Royal Society of London. Series B, Biological Sciences* 365, no. 1555: 3227–3246.
- Richardson, A. D., B. H. Braswell, D. Y. Hollinger, J. P. Jenkins, and S. V. Ollinger. 2009. "Near-Surface Remote Sensing of Spatial and Temporal Variation in Canopy Phenology." *Ecological Applications* 19, no. 6: 1417–1428.
- Richardson, A. D., J. P. Jenkins, B. H. Braswell, D. Y. Hollinger, S. V. Ollinger, and M. L. Smith. 2007. "Use of Digital Webcam Images to Track Spring Green-Up in a Deciduous Broadleaf Forest." *Oecologia* 152, no. 2: 323–334.
- Richardson, A. D., T. F. Keenan, M. Migliavacca, Y. Ryu, O. Sonnentag, and M. Toomey. 2013. "Climate Change, Phenology, and Phenological Control of Vegetation Feedbacks to the Climate System." *Agricultural and Forest Meteorology* 169: 156–173.
- Seyednasrollah, B., T. Milliman, and A. D. Richardson. 2019. "Data Extraction From Digital Repeat Photography Using xROI: An Interactive Framework to Facilitate the Process." *ISPRS Journal of Photogrammetry and Remote Sensing* 152: 132–144.
- Seyednasrollah, B., A. M. Young, K. Hufkens, et al. 2019. "Tracking Vegetation Phenology Across Diverse Biomes Using Version 2.0 of the PhenoCam Dataset." *Scientific Data* 6, no. 1: 222.
- Smith, A. M. 2018. "Forest Ecology in a Changing World: Effective Ground-Based Methods for Monitoring Temperate Broadleaved Forest Ecosystem Dynamics in Relation to Climate Change." PhD thesis, University of Plymouth, Plymouth.
- Soudani, K., N. Delpierre, D. Berveiller, et al. 2021. "A Survey of Proximal Methods for Monitoring Leaf Phenology in Temperate Deciduous Forests." *Biogeosciences* 18, no. 11: 3391–3408.
- Templ, B., E. Koch, K. Bolmgren, et al. 2018. "Pan European Phenological Database (PEP725): A Single Point of Access for European Data." *International Journal of Biometeorology* 62, no. 6: 1109–1113.
- Thornton, P. E., R. Shrestha, M. Thornton, S. C. Kao, Y. Wei, and B. E. Wilson. 2021. "Gridded Daily Weather Data for North America With Comprehensive Uncertainty Quantification." *Scientific Data* 8, no. 1: 190.
- Violle, C., B. J. Enquist, B. J. McGill, et al. 2012. "The Return of the Variance: Intraspecific Variability in Community Ecology." *Trends in Ecology & Evolution* 27, no. 4: 244–252.
- Vitasse, Y. 2013. "Ontogenic Changes Rather Than Difference in Temperature Cause Understory Trees to Leaf Out Earlier." *New Phytologist* 198, no. 1: 149–155.
- Wickham, H. 2016. *ggplot2: Elegant Graphics for Data Analysis*. New York: Springer-Verlag.
- Wingate, L., J. Ogeé, E. Cremonese, et al. 2015. "Interpreting Canopy Development and Physiology Using a European Phenology Camera Network at Flux Sites." *Biogeosciences* 12, no. 20: 5995–6015.
- Zanne, A. E., D. C. Tank, W. K. Cornwell, et al. 2014. "Three Keys to the Radiation of Angiosperms Into Freezing Environments." *Nature* 506, no. 7486: 89–92.
- Zohner, C. M., B. M. Benito, J. D. Fridley, J. C. Svenning, and S. S. Renner. 2017. "Spring Predictability Explains Different Leaf-out Strategies in the Woody Floras of North America, Europe and East Asia." *Ecology Letters* 20: 452–460.
- Zohner, C. M., L. Mo, and S. S. Renner. 2018. "Global Warming Reduces Leaf-Out and Flowering Synchrony Among Individuals." *eLife* 7: e40214.
- Zohner, C. M., L. Mo, S. S. Renner, et al. 2020. "Late-Spring Frost Risk Between 1959 and 2017 Decreased in North America but Increased in Europe and Asia." *Proceedings of the National Academy of Sciences of the United States of America* 117, no. 22: 12192–12200.

Supporting Information

Additional supporting information can be found online in the Supporting Information section.